Optical transition probabilities and compositional dependence of Judd–Ofelt parameters of Er^{3+} ions in fluoroindate glass

A. Florez[a,1], Y. Messaddeq[b], O.L. Malta[b,2], M.A. Aegerter[a]

[a] *Instituto de Física de São Carlos (IFSC), Universidade de São Paulo, C.P. 369 CEP 13560-970, São Carlos, SP, Brazil*
[b] *Instituto de Química da UNESP, C.P. 355, 14800-900 Araraquara, SP, Brazil*

Received 15 December 1994; in final form 27 February 1995

Abstract

Fluoroindate glasses containing 1, 2, 3, and 4 mol% ErF_3 were prepared in a dry box under an argon atmosphere . Absorption spectra of these glasses at room temperature were obtained. The Judd–Ofelt parameters Ω_λ ($\lambda = 2, 4, 6$) for f–f transitions of Er^{3+} ions as well as transition probabilities, branching ratios, radiative lifetimes, and peak cross-sections for stimulated emission of each band were determined. The concentration effect on the intensities is analyzed. The optical properties of the fluoroindate glasses doped with Er^{3+} ions are compared with those of other glasses described in the literature.

Keywords: Optical transitions; Judd–Ofelt parameters; Europium; Fluoroindate glass

1. Introduction

Since the discovery of fluoride glasses [1], there has been an increasing interest in the determination of the optical properties of heavy metal fluoride glasses doped with rare earths ions. A few years ago, it was found that InF_3-based systems have more stable compositions and better chemical properties [2] than other classes of glasses [3–5]. Their extended infrared transmission range (≈ 8 μm) [2,6], will allow the manufacture of optical fibers operating up to 5 μm, making possible the delivery of CO laser power. Devices based on rare earth ions in glasses, for example laser glasses, are characterized by absorption and emission probabilities which are influenced by the ligand field of the surrounding rare earth ions. Among the rare earth ions, Er^{3+} is one that has been studied the most since its laser oscillation is utilized as an optical fiber amplifier.

The Judd–Ofelt theory [7,8] is a useful theory for estimating the probability of the forced electric dipole transitions of the rare earth ions in various environments. In this theory of f–f transitions, the so-called intensity parameters Ω_2, Ω_4 and Ω_6 can be determined experimentally from the measurements of the absorption spectra and refractive index of the host material. From these parameters, several important optical properties, e.g., oscillator strengths, radiative transition probabilities, branching ratios, spontaneous emission coefficients and peak cross-sections for stimulated emission, can be evaluated. In the present paper, we have determined these quantities for the Er^{3+} ion as a dopant in fluoroindate glasses for several Er^{3+} concentrations.

2. Theory

In this work we have used the f–f intensity model described in detail elsewhere [9,10]. Thus, only a short summary and the most essential formulas will be given.

The oscillator strength is obtained from the area under the absorption band after transformation of the mean wavelength (λ) corresponding to the band baricenter to a convenient scale [11].

[1] In studies commission from the Departamento de Física, Universidad Industrial de Santander (UIS), A.A. 678, Bucaramanga, Colombia.

[2] On leave of absence from the Departamento de Química fundamental da UFPE, Cidade Universitaria, Recife, PE-50739, Brazil.

SSDI 0925-8388(95)01613-9

$$f = (4.318 \times 10^{-9}/Cl\lambda^2) \int K(\lambda)\, d\lambda \quad (1)$$

where $K(\lambda)$ is the spectral absorption coefficient, λ is in nm, and C and l are the concentration of Er^{3+} ions in mol $\times 1000$ cm^{-3} and the absorption path length, respectively.

From the f–f intensity model, the oscillator strength of a transition between two multiplets is given by

$$f = [8\pi^2 mc\sigma/3\hbar(2J+1)]\chi \times \sum_{\lambda=2,4,6} \Omega_\lambda \langle 4f^N(\alpha SL)J\|U^{(\lambda)}\|4f^N(\alpha'S'L')J'\rangle^2 \quad (2)$$

where m is the mass of the electron, c is velocity of light, h is Planck's constant, σ is the mean frequency for the transition, and χ is defined below.

The intensity parameters Ω_λ are determined from a least-squares fit to the values of the measured oscillator strengths, using Eq. (2), after the subtraction of the magnetic dipole contribution. The quality of the fit can be expressed by the magnitude of the root-mean-square (r.m.s.) deviation, defined by

$$\text{r.m.s.} = \left\{\sum (f_{\text{calc}} - f_{\text{Exp}})^2/(p-3)\right\}^{1/2} \quad (3)$$

where p is the number of parameters.

The total spontaneous emission probability between the J and J' levels is given by

$$A_{JJ'} = [64\pi^4\sigma^3/3\hbar(2J+1)](\chi S + \chi_{\text{md}} S_{\text{md}}) \quad (4)$$

where $\chi = n(n^2+2)^2/9$ and $\chi_{md} = n^3$ are the effective field corrections at a well-localized center in a medium of isotropic refractive index n. S and S_{md} are the electric dipole and magnetic dipole line strengths defined by

$$S = e^2 \sum_{\lambda=2,4,6} Q_\lambda \{f^N(\alpha SL)J\|U^{(\lambda)}\|f^N(\alpha SL)J'\rangle^2 \quad (5)$$

$$S_{\text{md}} = (e\hbar/4\pi mc)\langle f^N(\alpha SL)J\|\mathbf{L}+\mathbf{S}\|f^N(\alpha SL)J'\rangle^2 \quad (6)$$

The reduced matrix elements $\langle\|U^{(\lambda)}\|\rangle$ and $\langle\|\mathbf{L}+\mathbf{S}\|\rangle$ in the last two equations were obtained from Ref. [10]. $A_{JJ'}$ is related to the radiative lifetime τ_R of an excited state by

$$\tau_R = 1/\sum_{J'} A_{JJ'} \quad (7)$$

and the peak cross-section for stimulated emission, ρ_p, which is essential in predicting the laser perfomance, is given by

$$\rho_p = \lambda^4 A_{JJ'}/8\pi c n^2 \Delta\lambda \quad (8)$$

where λ is the average emission wavelength and $\Delta\lambda$ is the emission linewidth.

The branching ratio $\beta_{JJ'}$ corresponding to the emission from an excited J level to J' is

$$\beta_{JJ'} = A_{JJ'}/\sum_{J'} A_{JJ'} \quad (9)$$

3. Experimental

The fluoroindate glasses with bath compositions (mol%) of $20ZnF_2$–$20SrF_2$–$2NaF$–$16BaF_2$–$6GaF_3$–$(36-x)InF_3$ and $xErF_3$ with $x = 1$, 2, 3 and 4 were prepared. The mixtures were heated in a platinum

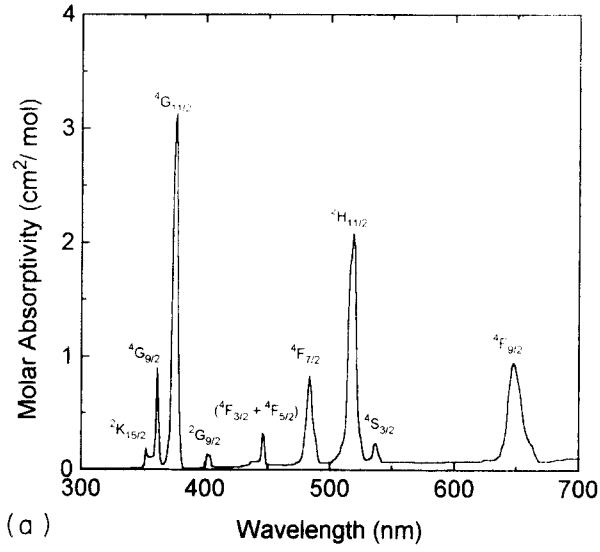

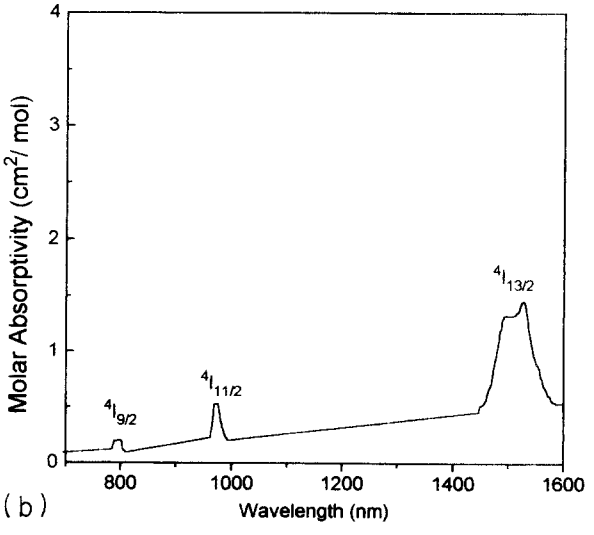

Fig. 1. Absorption spectrum of Er^{3+} in fluoroindate glass containing 1.0 mol% of Er^{3+}, at room temperature (a) from 300 to 700 nm and (b) from 700 to 1600 nm.

crucible at 800°C for 1 h for melting and 850°C for finish. Both heatings were performed in a dry box under an argon atmosphere. The melt was cast into a preheated mold at 260°C and slowly cooled up to room temperature. The samples were cut and polished into the shape of parallelepipeds. The refractive indices were measured using a refractometer (Pulfrich PR 2-Carl Zeiss/Jena), and a value of 1.49 was obtained for all samples. The density of the four samples varied between 4.8 and 5.0 g cm^{-3}, depending on the concentration.

The absorption spectra were recorded at room temperature using a CARY 17 spectrophotometer in the spectral range from 300 to 1600 nm. The absorption path lengths of the samples were 2.07 mm, 1.77 mm, 2.01 mm, and 1.43 mm for the concentrations 1, 2, 3, and 4 mol%, respectively. The CARY spectrophotometer provides a graph of $K(\lambda)$ as a function of the wavelength λ.

4. Results and discussion

Fig. 1. shows the absorption spectra of Er^{3+} ion in the fluoroindate glasses in the spectral range from 300 to 700 nm (a) and from 700 to 1600 nm (b) at room temperature. The hypersensitive transitions $^4I_{15/2} \rightarrow {}^2H_{11/2}$ and $^4I_{15/2} \rightarrow {}^4G_{11/2}$ can be identified from their intense absorptions. Also, it is important to note the complex aspect of the $^4I_{15/2} \rightarrow {}^4I_{13/2}$ transition. The spectra obtained for each sample show identical characteristics, while there is only a change in the intensity of the different bands as the concentration of Er^{3+} is changed.

For comparison, the energy level diagrams of the Er^{3+} free ion and the Er^{3+} ion in fluoroindate glass, obtained from the absorption spectra, are shown in Fig. 2. With the exception of small shifts, the energy

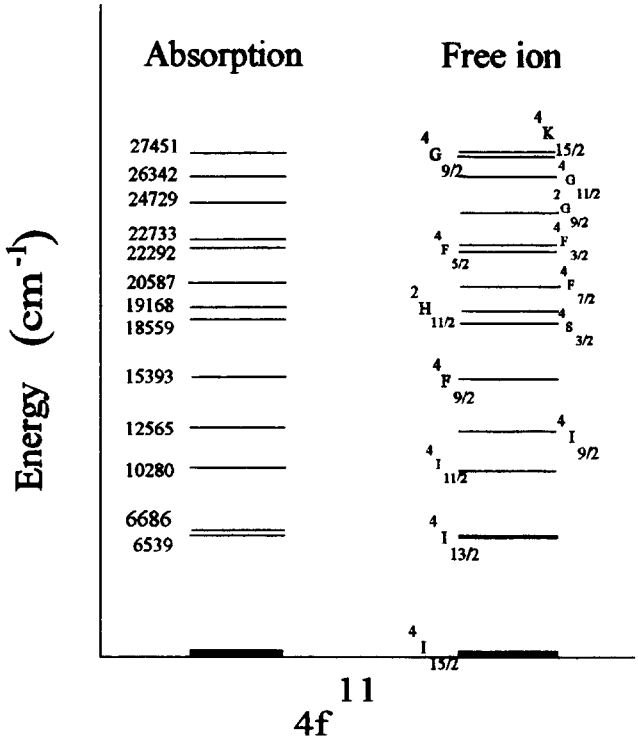

Fig. 2. Energy level diagram of Er^{3+} in fluoroindate glass, at room temperature, obtained from absorption spectra compared to reported [12] free ion levels (1 eV = 8065.479 cm^{-1}).

levels obtained for the Er^{3+} ion are in good agreement with those reported by Dieke [12] for the free ion.

The experimental and calculated oscillator strengths for the different samples are presented in Table 1. The excited J levels are given in column 1, and in the other columns are given the values of f_{exp} and f_{calc} (least-squares adjusted values) for each sample obtained from Eqs. (1) and (2). The average wavelengths were taken to be the baricenters of the absorption bands. From these results, it is noted that the oscillator strengths do not vary significantly with the concen-

Table 1
Comparison of experimental and calculated oscillator strengths, f, ($\times 10^6$) for absorption from the $^4I_{15/2}$ ground state of Er^{3+} ion in fluoroindate glass for different Er^{3+} concentrations

Upper state	1 mol%		2 mol%		3 mol%		4 mol%	
	exp	calc	exp	calc	exp	calc	exp	calc
$^4G_{9/2}$	2.13	1.65	1.53	1.36	1.31	1.35	1.13	1.27
$^4G_{11/2}$	8.14	7.92	8.03	7.77	7.52	7.22	7.83	7.58
$^2G_{9/2}$	0.56	0.55	0.64	0.68	0.62	0.62	0.59	0.66
$^4F_{3/2}$, $^4F_{5/2}$	0.76	0.63	1.05	0.86	0.81	0.77	0.86	0.86
$^4F_{7/2}$	1.56	1.67	1.95	1.87	1.73	1.75	1.89	1.83
$^2H_{11/2}$	4.15	4.52	3.98	4.43	3.58	4.09	3.86	4.31
$^4S_{3/2}$	0.40	0.33	0.234	0.46	0.27	0.41	0.324	0.46
$^4F_{9/2}$	2.05	2.35	1.91	2.03	2.03	1.99	1.99	1.91
$^4I_{9/2}$	0.32	0.43	0.26	0.30	0.30	0.31	0.34	0.27
$^4I_{11/2}$	0.40	0.38	0.55	0.51	0.52	0.46	0.54	0.51
$^4I_{13/2}$	1.00	0.95	1.07	1.19	1.10	1.09	1.17	1.18
r.m.s. =	0.26×10^{-6}		0.23×10^{-6}		0.22×10^{-6}		0.20×10^{-6}	

Table 2
Intensity parameters Ω_λ (in units of 10^{-20} cm^2) and spectroscopic quality factor Ω_4/Ω_6 of the Er^{3+} ion in the fluoroindate glass for different Er^{3+} concentrations

Concentration (mol%)	Ω_2	Ω_4	Ω_6	Ω_4/Ω_6
1	2.17	2.31	0.89	2.60
2	2.46	1.63	1.23	1.32
3	2.18	1.68	1.10	1.53
4	2.45	1.47	1.22	1.20

tration, showing that in this concentration range the doping effect on the intensities is small. The measure of the quality of the fit between the measured and calculated oscillator strengths is given by the r.m.s. deviation in the last row of Table 1. For the hypersensitive transitions $^4I_{15/2} \rightarrow {}^2H_{11/2}$ and $^4I_{15/2} \rightarrow {}^4G_{11/2}$ (Fig. 1(a)) the values obtained for the oscillator strength are smaller than those values reported by Reisfeld [9] in fluorozirconate and other fluoride glasses for equivalent concentrations. The r.m.s. deviation of the fitted values is smaller than that reported for fluorozirconate glass. This may be explained by the fact that in the fluoroindate glasses the hypersensitive transitions are weaker than in the other fluoride glasses [9,13]. The r.m.s value (0.20×10^{-6}) is lower for the 4.0 mol% sample and shows a small tendency to decrease from 1.0 to 4.0 mol%. Thus, the predictions of the f–f intensity model in this fluoroindate glass improve with increasing concentration up to 4 mol%.

Table 2 lists the three intensity parameters Ω_λ obtained by the least-squares fitting of the experimental oscillator strengths. Also included is the spectroscopic quality factor Ω_4/Ω_6 for all samples. The squared reduced matrix elements, $[U^{(\lambda)}]^2$, were taken from Ref. [10]. The value of each Ω_λ parameter varies only slightly with concentration. This variation is more pronounced in the Ω_4 and Ω_6 values, as can be noted in the 1 mol% sample which has a larger Ω_4/Ω_6 ratio. The similarity in the behaviour of the Ω_λ parameters in the samples with concentrations of 2, 3 and 4 mol% may be explained by the fact that the Er^{3+} ions are surrounded by similar environments. The hypersensitive transitions $^4I_{15/2} \rightarrow {}^2H_{11/2}$ and $^4I_{15/2} \rightarrow {}^4G_{11/2}$ are less affected by the inhomogeneity of the environment in these matrices than in other glasses [14]. The relatively small values of Ω_2 ($\approx 2.0 \times 10^{-20}$ cm^2) indicate the high degree of homogeneity of these glasses [15].

Table 3
Radiative transition probabilities, branching ratios, radiative lifetimes and peak cross-section of Er^{3+} ion in fluoroindate glass at room temperature

Transition	Average energy (cm^{-1})	$A_{JJ'}^{ed}$ (s^{-1})	$A_{JJ'}^{md}$ (s^{-1})	$\beta_{JJ'}$	τ_R (ms)	ρ_p (in units of 10^{-20} cm^2)
$^4I_{13/2} \rightarrow {}^4I_{15/2}$	6602	69.64	35.17	1.0000	9.54	0.4879
$^4I_{11/2} \rightarrow {}^4I_{15/2}$	10279	79.37		0.8593	10.83	0.2563
$^4I_{13/2}$	3677	3.63	9.37	0.1407		0.2386
$^4I_{9/2} \rightarrow {}^4I_{15/2}$	12612	159.57	0.8906	5.58	0.2328	
$^4I_{13/2}$	6010	17.27		0.0964		0.4810
$^4I_{11/2}$	2333	1.01	2.16	0.0177		0.3464
$^4F_{9/2} \rightarrow {}^4I_{15/2}$	15379	1307.2		0.8142	0.0623	1.1547
$^4I_{13/2}$	8777	243		0.1514		1.9989
$^4I_{11/2}$	5100	47.67		0.0297		3.4387
$^4I_{9/2}$	2767	7.61		0.0047		6.3495
$^4S_{3/2} \rightarrow {}^4I_{15/2}$	18552	674.06		0.7175	1.06	0.7218
$^4I_{13/2}$	11950	180.14		0.1917		1.1063
$^4I_{11/2}$	8273	59.77	0.0636		1.6004	
$^4I_{9/2}$	5940	22.13		0.0236		2.2319
$^4F_{9/2}$	3173	3.37		0.0036		4.1799
$^2H_{11/2} \rightarrow {}^4I_{15/2}$	19267	3295.5		0.6968	0.211	2.1767
$^4I_{13/2}$	12665	936.06		0.1979		3.2878
$^4I_{11/2}$	8988	334.56		0.0707		4.6366
$^4I_{9/2}$	6655	135.81		0.0287		6.2648
$^4F_{9/2}$	3888	27.08		0.0057		10.7420
$^4S_{3/2}$	715	0.17		0.0	58.8770	
$^4F_{7/2} \rightarrow {}^4I_{15/2}$	20592	2088.1		0.6601	0.316	1.3233
$^4I_{13/2}$	13990	654.81		0.2070		1.9312
$^4I_{11/2}$	10313	262.31		0.0829		2.6244
$^4I_{9/2}$	7980	121.52		0.0384		3.3993
$^4F_{9/2}$	5213	33.88		0.0107		5.2025
$^4S_{3/2}$	2040	2.03		0.0006		13.3060
$^2H_{11/2}$	1325	0.56		0.0002		20.4390

Table 3. *Continued*

Transition		Average energy (cm^{-1})	$A^{ed}_{JJ'}$ (s^{-1})	$A^{md}_{JJ'}$ (s^{-1})	$\beta_{JJ'}$	τ_R (ms)	ρ_p (in units of 10^{-20} cm^2)
$^4F_{3/2}$ $^4F_{5/2}$ →	$^4I_{15/2}$	22362	1230.5		0.6138	0.50	0.7227
	$^4I_{13/2}$	15760	430.75		0.2149		1.0417
	$^4I_{11/2}$	12083	194.12		0.0968		1.4023
	$^4I_{9/2}$	9750	101.99	0.0509		1.7964	
	$^4F_{9/2}$	6983	37.47		0.0187		2.6909
	$^4S_{3/2}$	3810	6.09		0.0030		6.2417
	$^2H_{11/2}$	3095	3.26		0.0016		8.8184
	$^4F_{7/2}$	1770	0.61		0.0003		38.5800
$^2G_{9/2}$ →	$^4I_{15/2}$	24692	794.63		0.5573	0.70	0.3265
	$^4I_{13/2}$	180.90	312.47		0.2192		0.4417
	$^4I_{11/2}$	14413	158.03	0.1108		0.5550	
	$^4I_{9/2}$	12080	93.05		0.0653		0.6627
	$^4F_{9/2}$	9313	42.64		0.0299		0.8605
	$^4S_{3/2}$	6140	12.22	0.0086		1.3074	
	$^2H_{11/2}$	5425	8.43		0.0059		1.4780
	$^4F_{7/2}$	4100	3.64		0.0025		1.9586
	$^4F_{5/2}$	2330	0.67		0.0005		3.4331
$^4G_{11/2}$ →	$^4I_{15/2}$	26457	10886		0.5182	0.048	3.0054
	$^4I_{13/2}$	19855	4601.4		0.2190		3.9556
	$^4I_{11/2}$	16178	2489.1		0.1185		4.8760
	$^4I_{9/2}$	13845	1560.1		0.0743	5.6930	
	$^4F_{9/2}$	11078	799.22		0.0380		7.1047
	$^4S_{3/2}$	7905	290.39		0.0138		9.9863
	$^2H_{11/2}$	7190	218.51		0.0104		10.9540
	$^4F_{7/2}$	5865	118.6	0.0056		13.4590	
	$^4F_{5/2}$	4095	40.37		0.0019		19.2760
	$^2G_{9/2}$	1764	3.23		0.0002		44.7290
$^4G_{9/2}$ →	$^4I_{15/2}$	27451	2919.3		0.4976	0.17ms	1.2264
	$^4I_{13/2}$	20849	1278.9	0.2180		1.5967	
	$^4I_{11/2}$	17172	714.61		0.1218		1.9445
	$^4I_{9/2}$	14839	461.13		0.0786		2.2435
	$^4F_{9/2}$	12072	248.28		0.0423		2.4423
	$^4S_{3/2}$	8899	99.46		0.0169		3.7514
	$^2H_{11/2}$	8184	77.36		0.0132		4.0777
	$^4F_{7/2}$	6859	45.54		0.0078		4.8667
	$^4F_{5/2}$	5089	18.60		0.0032		6.5751
	$^2G_{9/2}$	2758	2.96		0.0005		12.1080
	$^4G_{11/2}$	994	0.14		0.0		33.0740

The calculated magnetic dipole contributions to the observed intensities are very small except for the $^4I_{13/2} \rightarrow {}^4I_{15/2}$, $^4I_{11/2} \rightarrow {}^4I_{13/2}$ and $^4I_{9/2} \rightarrow {}^4I_{11/2}$ radiative transitions. In these cases, the magnetic dipole contributions are in agreement with those reported by Shinn et al. [16] for Er^{3+} in ZBLA glass [16].

Table 3 gives the energies of the possible $J \leftrightarrow J'$ transitions involving the eleven J levels obtained from the absorption spectrum of the sample with a concentration of 1 mol%, which has the highest spectroscopic quality factor ($\Omega_4/\Omega_6 = 2.60$). The quantities $A_{JJ'}$, $\beta_{JJ'}$, τ_R and ρ_p were calculated on the basis of Eqs. (6)–(9), respectively, and the results are included in Table 3. The values obtained for these quantities are comparable to those reported for other fluoride glasses [9,17].

5. Conclusions

We have investigated the reliability of the predictions of the f–f intensity model for Er^{3+} doped fluoroindate glass with different concentrations (1–4 mol%) at room temperature. This investigation supports this model remarkably well, as can be noted from the small r.m.s. deviations obtained, in comparison to similar results reported for other glasses.

The spectroscopic properties found from the absorption spectra of the Er^{3+} ion doped to fluoroindate glass are similar to other Er^{3+} ion doped glasses [9]. The small variation of Ω_2 with concentration may be associated with the micro-structural homogeneity around the Er^{3+} ions. The differences between the values of A'_{JJ} and $\beta_{JJ'}$ as determined here, and those

reported for the same parameters in other systems, may be due to the fact that in our investigation only electric dipole like transitions were considered, except for the $^4I_{13/2} \rightarrow {}^4I_{15/2}$, $^4I_{11/2} \rightarrow {}^4I_{13/2}$, and $^4I_{9/2} \rightarrow {}^4I_{11/2}$ transitions which have considerable magnetic dipolar contributions (Table 4).

Our analysis provides evidence that Er-doped fluoroindate glass has a higher degree of homogenity than other Er-doped glasses [14]. This, coupled with low phonon energies [15], makes Er-doped fluoroindate glass a promising material for use as a fiber laser or fiber amplifier.

Acknowledgments

This research was supported by Telebrás, Fapesp, Capes, CNPq program RHAE–New Materials, Brazil.

References

[1] M. Poulain, M. Poulain and J. Lucas, *Mater. Res. Bull., 10* (1975) 243.
[2] Y. Messaddeq and M. Poulain, *Mater. Sci. Forum, 67/68* (1989) 161.
[3] M. Bouaggad, *PhD Thesis*, University of Rennes, 1986.
[4] Y. Messaddeq, *PhD Thesis*, University of Rennes, 1990.
[5] Y. Messaddeq, A. Delben, M. Boscolo, M.A. Aegerter, A. Soufiane and M. Poulain, *J. Non-Cryst. Solids, 161* (1993) 210.
[6] T. Sugana, Y. Miyasima and T. Konuki, *Electron. Lett. 26* (1990) 2042.
[7] B.R. Judd, *Phys. Rev., 127* (1962) 750.
[8] G.S. Ofelt, *J. Chem. Phys., 37* (1962) 511.
[9] R. Reisfeld, G. Katz, N. Spector, C.K. Jorgensen, C. Jacoboni, R. De Pape, *J. Solid State Chem., 43* (1982) 253.
[10] W.T. Carnall, H. Crosswhite and H.M. Crosswhite, Energy level structure and transition probabilities of the trivalent lanthanides in LaF_3, 1977 (Argone National Laboratory Special Report).
[11] A.A. De Souza da Gama, *PhD Thesis*, UFPE (1981) 88.
[12] G.H. Dieke, *Spectra and Energy Levels of Rare Earth Ions in Crystals*, Interscience, New York, 1968.
[13] R.D. Peacock, *Struct. Bond., 22* (1975) 83.
[14] S. Tanabe, T. Ohyagi, N. Soga and T. Hanada, *Phys. Rev., B46* (1992) 3305.
[15] R. Reisfeld and C.K. Jorgensen, Excited state phenomena in vitreous materials, *Handbook on the Physics and Chemistry of Rare Earths*, Elsevier Science Publishers, 1987, Chapter 58.
[16] M.D. Shinn, W.A. Sibley, M.G. Drexhage and R.N. Brown, *Phys. Rev., B27* (1983) 6635.
[17] R. Reisfeld, G. Katz, C. Jacoboni, R. De Pape, M.G. Drexhage, R.N. Brown and C.K. Jorgensen, *J. Solid State Chem., 48* (1983) 323.
[18] M.J. Weber, *Phys. Rev., 157* (1967) 231.
[19] W.F. Krupke, *Phys. Rev., 145* (1966) 325.
[20] C.K. Jorgensen and B.R. Judd, *Mol. Phys., 8* (1964) 281.
[21] X. Zou and T. Izumitani, *J. Non-Cryst. Solids, 162* (1993) 68.
[22] W.T. Carnall, P.R. Fields and B.G. Wybourne, *J. Chem. Phys., 42* (1965) 3797.
[23] M.J. Weber, *Phys. Rev., B8* (1973) 47.
[24] G.M. Reufro, J.C. Windscheit, W.A. Sibley and R.F. Bett, *J. Lumin., 22.*
[25] M.D. Shinn, J.C. Windscheit, D.K. Sardar and W.A. Sibley, *Phys. Rev., B26* (1982) 2371.